

Encased Beam with Variable Upper Steel Flange Position

Ahmed Youssef Kamal

Civil Engineering Department, Benha Faculty of Engineering, Benha University, Egypt.

ABSTRACT

Encased beam composite construction employs structural members that are composed of two materials: structural steel (rolled or built-up) and reinforced concrete, is an example of composite members. Encased beams have been used as rigid reinforcement in deck bridges for several decades. Nowadays they are used mainly in railway reconstruction with limited building heights. In this paper the effect of the upper steel section flange position of encased beam on the beam capacity and beam ductility is analyzed. Three-dimensional non-linear finite element analysis adopted by ANSYS till failure is performed on twenty one simply supported encased concrete beams. For the purpose of validation of the finite element model developed, the numerical study is carried out on a simply supported concrete beam that was experimentally tested and reported in the literature; good agreement with the experimental results is observed. Specimens were tested under lateral loading. The test results indicate that the behavior of the beam is greatly affected by the steel beam upper flange position. Upper flange width the most important parameter influences the beam capacity and ductility is analyzed, some preliminary criteria for an adequate design are presented.

KEY WORDS: Encased, Beam, Upper, Flange, Position.

NOMENCLATURES

b : Concrete beam width.

b_s : Steel beam width.

ψ : Normalized width, defined as the steel beam width divided by the concrete beam width ($\psi = b_s/b$).

h_s :Steel beam height.

h_f : Top steel flange height from bottom steel flange.

η : Normalized height ($\eta = h_f/h_s$)

P_f : Failure load.

1.INTRODUCTION

Structural members that are composed of two materials: structural steel (rolled or built-up) and reinforced concrete are examples of composite members. Composite beams can take several forms; one of these forms is consisting of beams encased in concrete. In contrast with classical structural steel design, which considers only the strength of the steel, composite design assumes that the steel and concrete work together in resisting loads. The inclusion of the contribution of the concrete results in more economical designs, as the required quantity of steel can be reduced, in addition to both fire , corrosion protect achieved by concrete to steel section and drastically reduces the possibility of local buckling of the encased steel. Work on encased beams dates back to 1922 in the report of the National Physical Laboratory tests on filler joist panels [1]. Many researches followed for both fully and partially encased beams [2] - [5]. Two types of composite beams are addressed in AISC 2010, Chapter I [6]: fully encased steel beams which depend on the natural bond of concrete to steel for composite action and those beams with mechanical anchorage to the slab using headed stud shear connectors or other types of connectors (such as channels) which do not have to be encased. Ductility of the encased beam is very high that because of the high percentage of steel area and this is one of the favorable features for seismic construction, [7].

Breuninger [8] proposed an innovative composite cross section where the top flange of the steel beam is eliminated and the headed studs are directly welded to the web in the horizontal position. The headed studs in the horizontal position are called lying studs and experimental results showed that the load capacity is limited by: splitting of the concrete slab, and tear-off or pull-out of the studs. Parameters such as concrete strength, thickness of concrete slab, distance, diameter and length of the studs, number and diameter of the stirrups, and reinforcement of slabs showed to be very important [8]. An interesting slim floor system is proposed by Ju and Kim [9] to minimize story height and consists of inverted T-section steel beam and precast concrete rested on the bottom flange. Stirrups and lying studs on the top web are used to provide the composite action.

In other research, where reinforcing bars and headed shear studs were combined to provide the composite action, the longitudinal shear force transfer occurred mainly by friction forces acting at the interface among the concrete encasement and the structural steel [9]. Regarding the failure modes, the absence of the reinforcement or headed studs

leads to a failure without diagonal cracks. With reinforcing bars, the behavior becomes more ductile, and with headed studs, the failure is achieved by splitting the concrete around the studs [10]. The AISC LRFD Specification [6] permits two methods of design for encased steel beams. In the first method, the design strength of the encased section is based on the plastic moment capacity, of the steel section alone. In the second method, the design strength of the encased section is based on the first yield of the tension flange assuming composite action of the concrete that is in compression and the steel section. Either way, there is no need to consider local buckling or lateral-torsional buckling of the steel beam because such buckling is inhibited.

The present study here is coming to look for effect of both upper steel flange position and width on the beam ductility and capacity. In the present study, Ammar A., et al. [7], tested specimen is chosen to verify the applicability of ANSYS computer program to analyze the encased composite beams and also to investigate the main parameters that affected its behavior.

2.GEOMETRY AND MATERIAL PROPERTIES

Twenty simply supported encased beams, loaded by mid-span concentrated load divided into four groups (with variable normalized width α of 0.33, 0.5, 0.67 and 0.86), each group with variable normalized height β of (0, 0.25, 0.5, 0.75 and 1), in addition to control beam (reinforced concrete beam without steel section), are studied and analyzed.

An overall view of the model loaded with mid-span concentrated load is presented in Fig. (1). The beam test specimens had a square cross section of 150×150 mm, with beam total length of 1500 mm, and net length (distance between supports) of 1400 mm. The structural steel section used in the specimens was with height of 100 mm, constant for all models (0.67 of the concrete beam height), the steel section web and flange were with thickness of 3, and 5.7 mm respectively, and yield strength of 27.35 kg /mm². The centroids of both the structural steel shape and the geometric center of the concrete beam cross section are coincident [7].

All the beams were reinforced with two 12 mm diameter bars (high tensile steel) as tension and compression reinforcement. The yield strength of these longitudinal reinforcements was reported as 36 kg/mm². Closed stirrups with 6 mm diameter (mild steel) were placed at space of 200 mm center to center along the length of the beam to engage the longitudinal bars and to enhance the deformation ductility of the beam. The elastic modulus and Poisson's ratio for all reinforcements and steel section were considered as 20000 kg/mm² and 0.3, respectively, steel materials were simulated in the numerical model as bi-linear behavior. The concrete cover for the reinforcements at top, bottom and sides was taken as 10 mm. The compressive strength of concrete was considered as 3.13 kg/mm², with Poisson's ratio of 0.17 (as reported in Ammar A., et al. [7]).

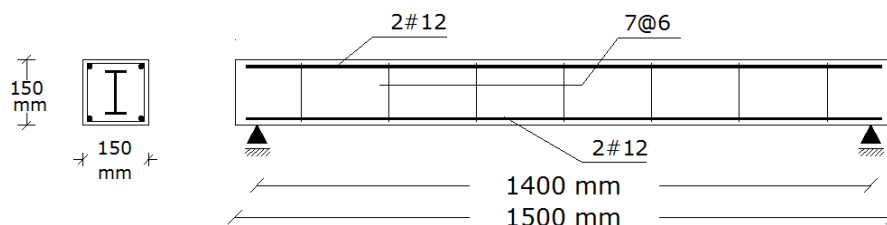


Figure (1) Overall view of the model.

3.NUMERICAL STUDY

Advances in computational features and software have brought the finite element method within reach of both academic research and engineers in practice by means of general-purpose nonlinear finite element analysis packages, with one of the most used nowadays being ANSYS. The finite elements adopted by ANSYS were used for this study. In the present study, the structural system modeling is based on the use of this commercial software. The finite element types considered in the model are as follows: elastic-plastic shell (SHELL43) and solid (SOLID65) elements for the steel section and the concrete, respectively. Both longitudinal and transverse reinforcing bars are modeled as discrete using (LINK8) element. Rigid-to-flexible contact mechanisms are used to model the interface contact surface between the structural steel section and the encased concrete. The rigid target surface (encased steel section which is represented by (SHELL43) element) modeled with (TARGE170) elements, while the contact flexible surface (concrete encasement which is represented by (SOLID65) elements) modeled with (CONTA173) elements. The element (SHELL43) is defined by four nodes having six degrees of freedom at each node. The deformation shapes are linear in both in-plane directions. The element allows for plasticity, creep, stress stiffening, large deflections, and large strain capabilities.

The element (SOLID65) is used for three dimensional modeling of solids with or without reinforcing bars (rebars capability). The element has eight nodes and three degrees of freedom (translations) at each node. The concrete is capable of cracking (in three orthogonal directions), crushing, plastic deformation, and creep. The concrete element

shear transfer coefficients considered are: 0.25 for open crack and 0.8 for closed crack. Typical values range from 0 to 1, where 0 represents a smooth crack (complete loss of shear transfer) and 1 a rough crack (no loss of shear transfer). The default value of 0.6 is used as the stress relaxation coefficient (a device that helps accelerate convergence when cracking is imminent). The crushing capability of the concrete element is also disabled to improve convergence.

The rebars (LINK8) element are capable of sustaining tension and compression forces, but not shear, being also capable of plastic deformation and creep and have two nodes with three translation degrees of freedom at each node. The bond between steel reinforcement and concrete was assumed to be perfect and no loss of bond between them was considered in this study [11-13]. The Link 8, 3-D spar element for the steel reinforcement was connected between nodes of each adjacent concrete Solid 65 elements so that the two materials share the same nodes. Due to symmetric shape the finite element models were represent the quarter actual model.

Good match was obtained between the experimental and finite element model, based on that the previous element will be used in this study.

4.Verification of the developed model

The results of the developed numerical model using the nonlinear finite element program ANSYS was calibrated against experimental data reported by Ammar A., et al. [7]. The goal of the comparison of the finite element models and the beam experimental work is to ensure that the elements types, meshing, material properties, real constants and convergence criteria are adequate to model the response of the beams, the comparisons are given below in Figure 2. Figure 2 shows the vertical deflection at beam mid-span versus load for beam with normalized width (ψ) and normalized height (η) of 0.33 and 1 respectively (I-section). The figure clearly demonstrates that the model is capable of predicting the deflection– load relationship (the same behavior) of the investigated beam with good accuracy. For both experimental and finite element models, the same type of concrete cracks (flexural cracks) initially occurred at load of 4080, 4300 kg respectively; afterwards, the cracks progressively grew till failure. The finite element model indicates the same failure mode (flexure failure) as the experimental one, with difference in failure load level of 10 %. It is obvious from pervious that the results from finite element model are in good agreement with the experimental data. It is now, strongly believed that the developed model provides good opportunity to outline trends in the behavior of encased beam as affected by different parameters. The model is therefore used in the coming section to study the pre-selected variables affecting the performance of the encased beam.

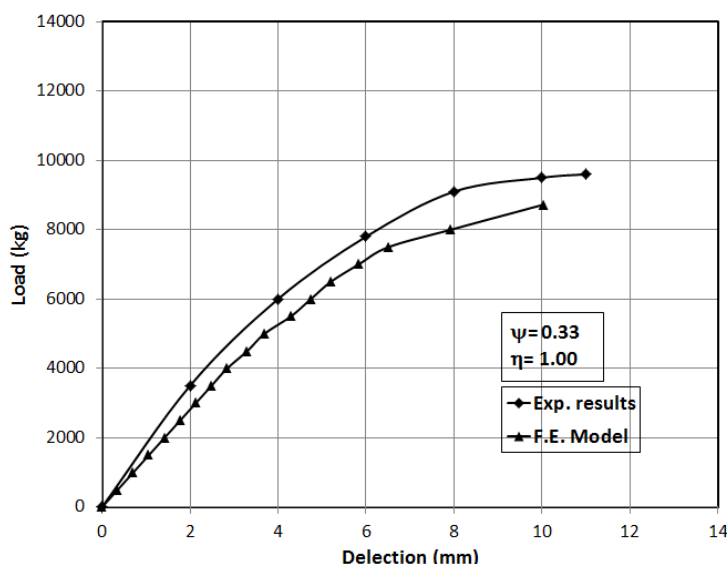


Figure (2) Verification of developed model.

5.RESULTS AND DISCUSSIONS

The deflected shapes for encased beam with both (I-section and inverted T-section), for different normalized width (ψ) of (0.33 and 0.86) at the same load level (within linear stage), are compared with control beam to indicate the beam ductility, as shown in Figure 3. The figure shows that encased beam in general is more ductile than reinforced concrete beam, as that the encased beam with steel I-section is more ductile than encased beam with inverted steel T-section. Figure also shows that increasing the normalized width (ψ) improve the beam ductility.

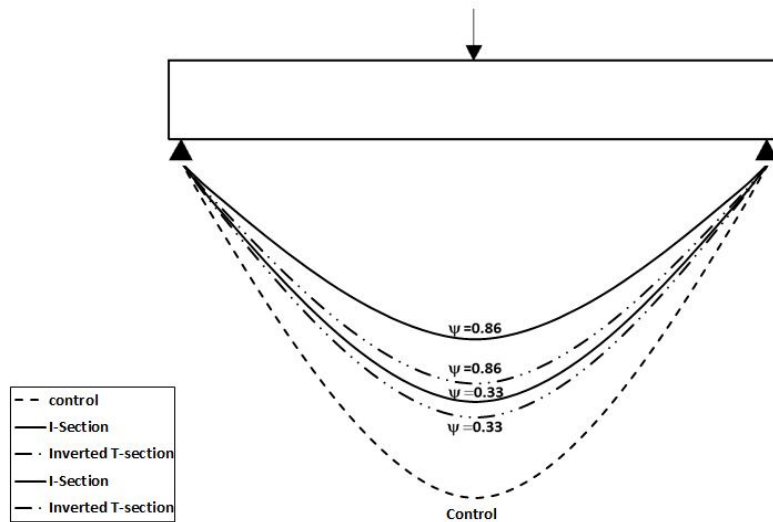


Figure (3) Beam deflected shape.

The mid-span vertical deflection at different load levels with various normalized width (ψ) and height (η) is compared with control beam to indicate the beam behavior. This comparison is done through (deflection –load) curves, as shown in Figure 4. Curves show that increasing in the normalized width (ψ), improve the beam deflection by increasing the beam ductility for all values of various normalized height (η).

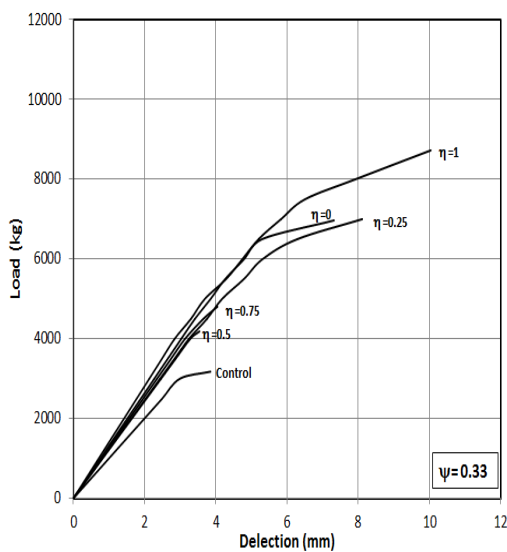


Figure 4.a

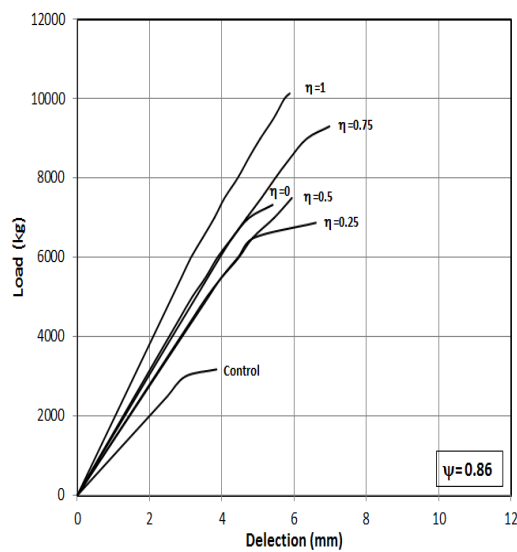


Figure 4.b

Figure (4) Deflection- load curves

For normalized height ($\eta=1, 0.75, 0.5, 0.25, 0$) the decrease in mid-span vertical deflection increase from (30, 20, 20, 20, 25 %) at ($\psi =0.33$) to (48, 37, 29, 29, 34 %) respectively, compared to that of control beam at the same load level, this is an expected behavior; due to increase in the steel section inertia result in deflection reduction. From previous the more affected normalized height by increasing the normalized width (ψ), was for ($\eta=1$) this is due to the symmetrical shape which keep approximately the neutral axis in the same position so the change in inertia play more effective role. On the other hand the less affected normalized height by increasing the normalized width (ψ) was for ($\eta=0$), this due to the concentration of steel area downward which push the neutral axis to be more toward the steel area result in limited increase in inertia. For all values of normalized width (ψ), moving the steel upper flange away from the natural axis result in high reduction in deflection as recorded for ($\eta=1, 0$) (I-section and inverted T-section) the reduction was (40, 30 %) in average respectively, otherwise the lowest deflection reduction was recorded at ($\eta=0.5, 0.25$) with average value of 25% compared to that of control beam at both load level and normalized width (ψ).

Figure 5 shows the models concrete cracks initiation level for models with steel (I-section and inverted T-section). For normalized width ($\psi=0.33$) concrete cracks initiated approximately at the same load level for all values of various normalized height (η) but with different type. For normalized height of ($\eta=1$) flexural cracks initially occurred at load of 4300 kg ($0.5 P_f$) afterwards, the cracks progressively grew till failure, with initiation of concrete crushing in the compression zone at load level of 5000 kg ($0.57 P_f$). While for models with normalized height of ($\eta=0.75, 0.5, 0.25$), flexural cracks and concrete crushing in the compression zone initially occurred simultaneously at the same load level of 4300 kg ($0.9, 1, \text{ and } 0.6 P_f$) respectively. For normalized height of ($\eta=0$) crushing in the compression zone first initially occurred at load level of 4300 kg ($0.6 P_f$), and after that flexural cracks initially at load level of 5000 kg ($0.72 P_f$) afterwards the cracks progressively grew till failure.

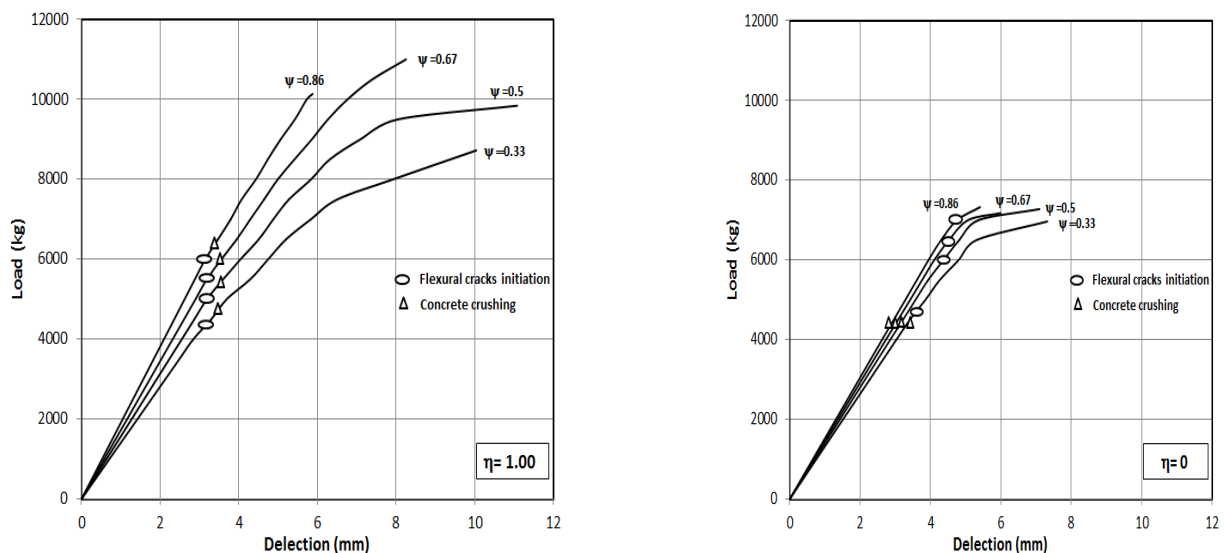


Figure (5.a) Encased beam with steel (I-section). **Figure (5.b)** Encased beam with steel (inverted T-section).

Figure (5) Concrete cracks initiation.

For normalized width ($\psi=0.86$) concrete cracks initiated at different load level and with different type for various normalized height (η). For normalized height of ($\eta=1$) flexural cracks initially occurred at load of 6000 kg ($0.5 P_f$) afterwards, the cracks progressively grew till failure, with initiation of concrete crushing in the compression zone at load level of 6500 kg ($0.64 P_f$). While for normalized height of ($\eta=0.75, 0.5, 0.25, 0$), crushing in the compression zone initiated first at load level of (5000, 4300, 4300, and 4300) kg ($0.6 P_f$) respectively, and after those flexural cracks initially at load level of (5500, 5500, 6000, and 7000) kg ($0.6, 0.73, 0.87, 0.95 P_f$) respectively, afterwards the cracks progressively grew till failure.

For normalized height ($\eta=1$) (I-section), flexural cracks initially occurred at load level of (4300, 5000, 5500, 6000) kg, for normalized width ($\psi=0.33, 0.5, 0.67, 0.86$) respectively; ($0.5 P_f$) approximately; afterwards, the cracks progressively grew till failure, with initiation of concrete crushing in the compression zone at load level (5000, 5500, 6000, 6500) kg, for normalized width ($\psi=0.33, 0.5, 0.67, 0.86$) respectively, as shown in Figure 4.a. It can be seen also that the beam is showing linear behavior until (4300, 5000, 5500, 6000) kg; for normalized width ($\psi=0.33, 0.5, 0.67, 0.86$) respectively, as the flexural cracks initiated, afterwards, the nonlinearity of the curves began.

For normalized height ($\eta=0$) (inverted T-section), concrete crushing in the compression zone initially occurred at load level of 4300 kg ($0.6 P_f$) for all normalized width values, with flexural cracks initiation at load level of (5000, 6000, 6500, 7000) kg, ($0.72, 0.82, 0.9, 0.95 P_f$) for normalized width of ($\psi=0.33, 0.5, 0.67, 0.86$) respectively, afterwards, the cracks progressively grew till failure, as shown in Figure 4.b. It can be seen also that the beam is showing linear behavior until (4300, 5000, 5500, 6000) kg; for normalized width ($\psi=0.33, 0.5, 0.67, 0.86$) respectively, as the flexural cracks initiated, afterwards, the nonlinearity of the curves began. From previous using encased beam with inverted steel T-section, delays the initiation of the flexural concrete cracks by 20 % in average comparing with that with I-section for all values of normalized width. While using encased beam with I-section delays the initiation of concrete crushing by (16, 28, 40, and 50 %) comparing with that with inverted steel T-section.

The Failure mode of all models was flexural failure, for normalized height of ($\eta=1, 0.75, 0.5$) the failure load increased from (8724.8, 4806.4, 4187.6) kg at normalized width of ($\psi=0.33$), to (10137.6, 9306.4, 7500) kg at normalized width of ($\psi=0.86$) respectively, which mean that there was increase in the failure load by (17, 94, 80) %. While for

normalized height of ($\eta=0.25, 0$) there was no significant change in the failure load by increasing the normalized width from ($\psi=0.33$ to 0.86). The failure load for the encased beam with steel I-section was higher than that with inverted T-section by (25, 35, 58, 35) %, for normalized width of ($\psi=0.33, 0.5, 0.67, 0.86$) respectively, as shown in Figure 6.

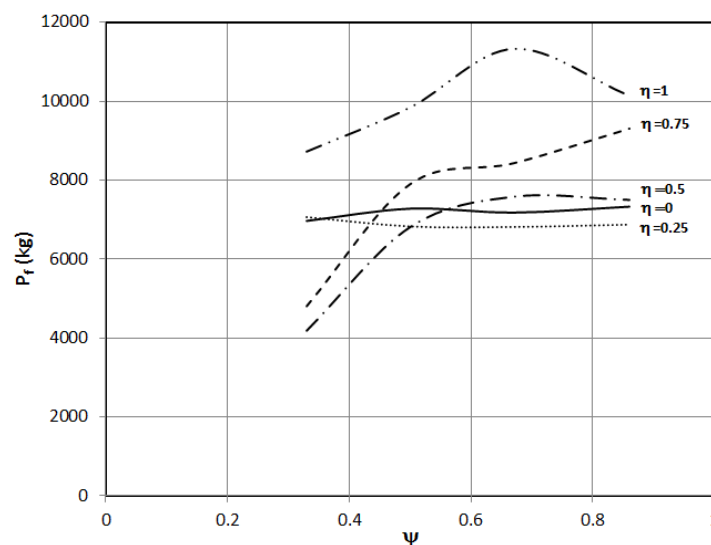


Figure (6) Failure loads.

6. CONCLUSIONS

A finite element analysis has been carried out to study the effect of the upper steel section flange position and width for encased beam. Based on the results obtained from the numerical study, the major conclusions drawn are summarized below.

- Ductility of the encased beam is very high.
- Increasing the steel section flange width resulted in more beam ductility.
- Encased beam with steel I-section (symmetric shape) is more ductile than that with inverted T-section (un-symmetric), for the same steel flange width.
- The nonlinearity behavior of the encased beam begins with the first flexural concrete cracks Initiations.
- Existence of the upper steel flange near the compression zone, delays the initiation of concrete crushing, as the moving of the upper steel flange toward the tension zone delays the initiation of flexural concrete cracks.
- Increasing the steel section flange width has no significant effect on the beam failure load of beam with inverted T-section.
- The failure load level for the encased beam with steel I-section is higher than that with steel inverted T-section.

REFERENCES

- [1] Adekola, A.O., "Elastic and plastic behaviour of cased beams", Build. Sci. Vol.2, pp. 321-330, Pergamon Press 1968, Printed in Great Britain.
- [2] Kindmann, R. and Bergmann, R., "Effect of reinforced concrete between the flanges of the steel profile of partially encased composite beams", J. Construct. Steel Research, 27, 107-122, 1993.
- [3] Roeder, C.W., Chmielowski, and Brown, C.B., "Shear connector requirements for embedded steel sections", ASCE Journal of Structural Engineering, Vol. 125, No. 2, February, 1999.
- [4] Hegger, J. and Goralski, C., "Structural behavior of partially concrete encased composite sections with high strength concrete", In: Composite construction in steel and concrete V: proceedings of the 5th international conference, Structural Engineering Institute of the American Society of Civil Engineers. Reston, VA: American Society of Civil Engineers, 2006.
- [5] Elghazouli, A.Y. and Treadway, J., "Inelastic behaviour of composite members under combined bending and axial loading", Journal of Constructional Steel Research 64, 1008–1019, 2008.
- [6] AISC, Specification for Structural Steel Buildings, American Institute of Steel Construction, Chicago, IL., 2010.
- [7] Ammar A., Saad N., and Wael S., "Strength and Ductility of Concrete Encased Composite Beams", Eng. and Tech. Journal, Vol. 30, No. 15, 2012.

- [8] Breuninger U. Design of lying studs with longitudinal shear force. In: International Symposium on connections between steel and concrete; 2001. p.1015–24.
- [9] Ju Y-K, Kim S-D. "Structural behavior of alternative low floor height system using structural Tee, half precast concrete, and horizontal stud". Canadian J. Civil Engineering 2005;32(2):329–38.
- [10][10] Hegger J, Goralski C. " Structural behavior of partially concrete encased composite sections with high strength concrete". In: 5th international conference in composite construction in Steel and concrete. South Africa; 2005, p. 346–55.
- [11] Swanson Analysis Systems, ANSYS. Online manual, (2005) and Theory Reference.10th ed. Swanson Analysis Systems, s.l., s.d.
- [12] Raad K. Shukur, "Nonlinear Analyses of Partially Composite Steel Beam Encased in Concrete with Innovative Position of Stud Bolts", Journal of Engineering, Volume 15 march 2009.
- [13] Ahmed Youssef, Ehab Hosny (2011), "Strengthening of R.C Beam with Openings by Near Surface Mounted CFRP: Experimental study", Engineering Research Journal 129, (2011).

AUTHOR



Ahmed Youssef received the B.S. and M.S. degrees in Civil Engineering from Benha Faculty of Engineering Benha University, Egypt, in 1995 and 2001, respectively. Also he received the Doctor OF Philosophy Degree in Structural Engineering from Faculty of Engineering - Zagazig University, Egypt, in 2005. During 2006 - 2011, he stayed in Benha Faculty of Engineering – Egypt as assistant professor, and during 2011-2015 he worked in Baha Faculty of Engineering- K.S.A. as assistant professor.